https://doi.org/10.5194/acp-2022-706
Preprint. Discussion started: 16 November 2022

Atmospheric Chemistry and Physics Discussions

Large Simulated Future Changes in the Nitrate Radical Under the CMIP6 SSP Scenarios: Implications for Oxidation Chemistry

Scott Archer-Nicholls[1,*], Rachel Allen[1], Nathan L. Abraham[1,2], Paul T. Griffiths[1,2], Alex T. Archibald[1,2]

[1]Department of Chemistry, University of Cambridge, Cambridge, CB2 1EW, UK
[2]NCAS-Climate, University of Cambridge, Cambridge, CB2 1EW, UK

*Now at IT Services, University of Manchester, Manchester, M13 9PL, UK

Correspondence to: Alex T. Archibald (ata27@cam.ac.uk)

Abstract. The nitrate radical (NO_3) plays an important role in the chemistry of the lower troposphere, acting as the principle oxidant during the night. Previous model simulations suggest that the levels of NO_3 have increased dramatically since the pre-industrial. Here, we show projections of the evolution of the NO_3 radical from 1850-2100 using the UKESM1 Earth System model under the CMIP6 SSP scenarios. Our model results highlight diverse trajectories for NO_3, with some scenarios and regions undergoing rapid growth of NO_3 to unprecedented levels over the course of the 21st Century, and others seeing sharp declines. The local increases in NO_3 are driven not only by local changes in emissions of nitrogen oxides but have an important climate component, with NO_3 being favoured in warmer future climates. The changes in NO_3 lead to changes in the oxidation of important secondary organic aerosol precursors, with potential impacts to particulate matter pollution regionally and globally. This work highlights the potential for substantial future growth in NO_3 and the need to better understand the formation of SOA from NO_3 to accurately predict future air quality and climate implications.

1 Introduction

Whilst nitrogen is ubiquitous in the atmosphere, the majority of gaseous nitrogen-containing molecules are chemically inert. Reactive nitrogen species (NO_y) make up a much smaller fraction but encompass a diverse set of molecules that play a paramount role in the chemistry of the atmosphere. Nitrogen oxide (NO) and nitrogen dioxide (NO_2), collectively known as NO_x, are essential for the catalytic formation of ozone (O_3) in the troposphere, a key air pollutant and greenhouse gas (Monks et al., 2015). The reaction of NO_2 with O_3 rapidly produces the nitrate radical (NO_3):

$$O_3 + NO_2 \rightarrow NO_3 + O_2 \quad (1)$$

During the daytime, NO_3 can undergo rapid photolysis or reaction with NO resulting in a very short lifetime; typically in the order of seconds (Wayne et al., 1991). However, at nighttime NO_3 is able to persist and become the major oxidant of volatile organic compounds (VOCs) (the hydroxyl radical (OH) and ozone (O_3) dominate this oxidation during the daytime); acting as

https://doi.org/10.5194/acp-2022-706
Preprint. Discussion started: 16 November 2022

Atmospheric Chemistry and Physics Discussions

the most important oxidant during the night (Brown and Stutz, 2021). NO_3 also undergoes a reversible reaction with NO_2, forming a thermal equilibrium with dinitrogen pentoxide (N_2O_5):

$$NO_2 + NO_3 + M \rightleftharpoons N_2O_5 + M, \quad (2)$$

$$K_{eq} = \frac{[NO_2][NO_3]}{[N_2O_5]} \quad (3)$$

N_2O_5 has a short lifetime with respect to decomposition at typical atmospheric boundary layer temperatures. As temperature increases, the rate of decomposition of N_2O_5 increases resulting in a greater fraction of reactive nitrogen in the form of NO_3. Due to their tight chemical-coupling, NO_3 and N_2O_5 have been termed the N_xO_y family (N_xO_y=NO_3+N_2O_5) (Stone et al., 2014). In this sense, sinks of N_2O_5 lead to corresponding indirect loss of NO_3. Loss of N_xO_y has important implications for tropospheric ozone as it is an important nighttime reservoir of NO_x and O_x (O+O_3+NO_2+others) (Archibald et al., 2020a). In the daytime, any remaining N_xO_y is converted back to NO_x, therefore nighttime sinks of N_xO_y reduce the levels of NO_x available to photochemically form ozone in the troposphere. The heterogeneous hydrolysis of N_2O_5, which occurs readily on aerosol surfaces, is one of the major nighttime sinks of reactive nitrogen in the troposphere (e.g., Riemer et al., 2003).

NO_3 reactions with alkenes proceed rapidly via addition of NO_3 to the double bond (Wayne et al., 1991, Brown and Stutz, 2012). As a result, the oxidation of biogenic volatile organic compounds (BVOCs), in particular terpenes that are emitted in vast quantities by the world's forests (Sakulyanontvittaya et al., 2008), is sensitive to the levels of NO_3 present (Ng et al., 2017). BVOC oxidation by NO_3 can lead to the formation of secondary organic aerosol (SOA) (Fry et al., 2009; Ng et al., 2017), fine aerosols that have implications for the planetary radiation budget and human health (Pöschl 2005). The extent that NO_3 initiated chemistry contributes to SOA formation (relative to O_3 and OH initiated production) depends on the molecular structure of the BVOC (and therefore their rate coefficients for reaction with NO_3), the rate of their emissions, and the levels of NO_3 present.

Ng et al. (2017) highlight that there are significant gaps in our understanding of the NO_3 initiated oxidation of BVOCs. BVOC oxidation chemistry has been studied for many decades (e.g., Brewer et al., 1984), however there are relatively few mechanistic studies of the products of NO_3 initiated oxidation (e.g., Boyd et al., 2015; Fry et al., 2009; Faxon et al., 2018, Ehn et al., 2017) compared to OH and O_3 (e.g., Atkinson and Arey, 2003; McGillen et al., 2020). Nonetheless there is mounting evidence that NO_3 oxidation could be a significant contributor to SOA formation. Kiendler-Scharr et al., (2016) highlight the ubiquity of organic nitrates in submicron aerosol collected in European nighttime urban conditions, whilst Hamilton et al., (2021) recently found NO_3 oxidation of isoprene to be a significant source of SOA production in Beijing. Recent studies show highly oxidised molecules (HOMs), formed from the autooxidation and accretion of monoterpene oxidation products, are capable of nucleating new aerosol particles without sulphate seeds (Ehn et al., 2014, Trostl et al., 2016, Bianchi et al, 2019) with important

https://doi.org/10.5194/acp-2022-706
Preprint. Discussion started: 16 November 2022


Atmospheric Chemistry and Physics Discussions

implications for large-scale feedbacks between the climate and the biosphere (Scott et al., 2017, Gordon et al., 2017). Recently, Zhao et al. (2021) have shown that HOMs from NO_3 initiated oxidation of isoprene may contribute to a significant fraction of the isoprene SOA yield. But these complex processes are so far lacking from Earth system and global chemistry-transport models.

Oxidation of BVOCs is dependent on changes to the oxidant budget (with respect to OH, O_3 and NO_3) and to the changes in the emissions of BVOCs themselves. Our understanding of the processes which control emissions of BVOCs highlights that these have important dependences on climatic parameters including CO_2 concentrations (Arneth et al., 2007), land use, temperature, humidity and precipitation (Arneth et al., 2008). Whilst BVOC emissions models are reasonably well constrained in the present day, past and future trends are less certain, with some models indicating large increases in BVOC emissions in the future (Pacifico et al., 2012) and others small to none (Hantson et al., 2017).

Estimates of changes in the levels of NO_3 from the pre-industrial to the present day indicate significant increases, on the order of 100-1000% (Khan et al., 2015), driven by changes in emissions of NO_x. Formation of NO_3 is also dependent on ozone burdens which are likely to change in the future (Archibald et al., 2020a; Griffiths et al., 2021). In addition, the fraction of N_xO_y in the form of NO_3 increases with temperature, while the main sinks are determined by the amount of N_2O_5 which decreases with temperature. Ng et al., (2017) postulated that NO_3 would increase with increasing NO_x emissions but given the complex chemical processes at work NO_3 is likely to vary nonlinearly with NO_x emissions. To our knowledge, no study has investigated how the NO_3 radical may change in the future under changing NO_x emissions and a changing climate, or how these changes will affect BVOC oxidation and SOA formation given changing terpene emissions.

This study presents results on the historic and future evolution of NO_3 using simulations from 1850-2100 made with the United Kingdom Earth System model (UKESM1) (Sellar et al., 2019, Archibald et al., 2020b). The simulations, based on the Coupled Model Intercomparison Project Phase 6 (CMIP6) Historic and ScenarioMIP scenarios (O'Neill et al., 2016), indicate that there are substantial changes in NO_3 simulated in the future at both the global mean and regional level, depending on the emissions scenarios and resulting climate considered. Using these simulations we show that future trends in NO_3 have an impact on the regional oxidation of BVOCs and as a result the SOA budget and burden. Taking a particular focus on changes occurring over South Asia, a region with severe present day air quality issues and large variation in how emissions will evolve in this region under different scenarios, we highlight an important role for enhanced levels of NO_3 initiated BVOC oxidation in the future.

2 Methods

2.1 Description of UKESM1 model

https://doi.org/10.5194/acp-2022-706
Preprint. Discussion started: 16 November 2022


Atmospheric Chemistry and Physics Discussions

The model simulations make use of the new U.K. Earth System Model (UKESM1) (Sellar et al., 2019). This is a fully coupled Earth system model using the Global Atmosphere 7.1/Global Land 7.0 (GA7.1/GL7.1; Walters et al., 2019). The dynamical model is coupled with the United Kingdom Chemistry and Aerosol model (UKCA), using the StratTrop mechanism for gas-phase chemistry (Archibald et al., 2020b) and the two-moment GLOMAP-mode aerosol scheme (Mulcahy et al., 2021). UKCA and UKESM1 are designed to quantify the response of the Earth system to forcings and simulate nascent feedbacks that exist in the coupled chemistry-aerosol-climate system. As such, pragmatic decisions have been made to ensure as complete a representation as possible of many processes are included in the model. For the chemistry of N_2O_5 this includes a fairly basic description of its chemistry in the gas phase and it's loss to aerosol surfaces (heterogeneous chemistry) is simplified, with a fixed uptake coefficient being used (γ=0.1). Jones et al. (2021) suggest that the simplified treatment of heterogenous uptake of N_2O_5 leads to an overestimate of the loss of N_2O_5 based on comparison of modelled and measured HNO_3 across the USA. UKCA does not include any in-particle chemistry for N_2O_5 and also lacks aerosol nitrate in the present implementation, similar to some other CMIP6 class models. The omission of aerosol nitrate is a weakness in the model but recent work including this process (Jones et al., 2021) suggests that the effects of it are small on N_xO_y.

The experimental setup is that of the simulations conducted as part of the Coupled Model Intercomparison Project Phase 6 (CMIP6; Eyring et al., 2016) DECK and ScenarioMIP experiments. Historical emissions are from the Community Emissions Data System (CEDS; Hoesly et al., 2018). Future emissions progress along one of four benchmark shared socioeconomic pathways (SSPs; Gidden et al., 2019). The analysis focuses on four representative pathways, SSP1-2.6, SSP2-4.5, SSP3-7.0 and SSP5-8.5. Each SSP has different assumptions about the amount of emissions of air pollutant precursors and climate forcers (reference changes in emissions of NO_x under the scenarios (Gidden et al., 2019)). We perform our analyses focused on 5 year periods (Preindustrial, PI: 1850-54; Present day, PD: 2010-14; end of century 2090-94). These were conducted by performing new simulations using re-start files from the start dumps from the core CMIP6 simulations contributed by UKESM1. It was necessary to re-run the CMIP6 simulations with UKESM1 in order to (i) provide high temporal resolution output with additional diagnostics for the NO_3 reactions which did not exist in the CMIP6 runs, needed to assess the oxidation of Monoterp and isoprene and (ii) include a correction to the NO_3+Monoterp reaction rate coefficient.

2.2 Description of relevant chemical reactions

The representation of BVOC chemistry in the Strat-Trop chemical mechanism used in the UKESM1 model is similar to other Earth system models in being very simplified. Isoprene is treated as an individual compound undergoing reactions with OH, O_3 and NO_3, while monoterpenes are represented with a surrogate species, Monoterp, which can undergo oxidation via OH, NO_3 or O_3 with rate coefficients equal to the equivalent oxidation reactions of -pinene to form an inert species, SEC_ORG, which irreversibly condenses to form SOA (Mann et al., 2010). This simplification has been shown to broadly capture the relation between BVOC emissions, SOA formation and the climate impacts well (Scott et al., 2017, Mulcahy et al., 2020).

https://doi.org/10.5194/acp-2022-706
Preprint. Discussion started: 16 November 2022


Atmospheric Chemistry and Physics Discussions

All monoterpenes are represented by the "Monoterp" species, which undergoes oxidation via OH, O_3 and NO_3 to form the "SEC_ORG" species, which in turn undergoes irreversible condensation to form secondary organic aerosol (SOA):

$$\text{Monoterp} + \text{OH} \rightarrow \text{F} * \text{SEC\_ORG};\ k_{OH}$$
$$\text{Monoterp} + \text{O}_3 \rightarrow \text{F} * \text{SEC\_ORG};\ k_{O3}$$
$$\text{Monoterp} + \text{NO}_3 \rightarrow \text{F} * \text{SEC\_ORG};\ k_{NO3}$$

Where F is some factor between 0 and 1 representing the yield of SOA production from MONOTERP. The assumed yield of SEC_ORG from Monoterp is 0.13, but is doubled to 0.26 in order to account for the missing production from isoprene oxidation (Mann et al., 2010, Mulcahy et al., 2020). The rate coefficients k_{OH}, k_{O_3} and k_{NO_3} are equal to the rate coefficients for the reactions between α-pinene and OH, O_3 and NO_3 respectively from Atkinson et al. (1989). Due to an error, the reaction rate coefficient activation energy for the NO_3+Monoterp reaction was incorrect in the original version of UKESM1 and has been corrected for these experiments. The rate coefficient used in all previous studies using StratTrop with GLOMAP aerosol was:

$$k_{NO_3} = 1.19 \times e^{(925/T)}$$

Whereas the correct form is:

$$k^*_{NO_3} = 1.19 \times e^{(490/T)}$$

At *T=298K*, this difference in activation energy results in k_{NO_3} being 4.3 times faster than $k^*_{NO_3}$. This correction results in a smaller fraction of Monoterp being oxidised by NO_3 compared to OH and O_3, partly compensated by an increase in NO_3 burden (see Supplement further details).

3 Results

3.1 Comparison of Present day modelled and observed NO_3.

Our analysis begins by evaluating the performance of UKESM1 against aircraft observations and pre-compiled ground-based observations presented in Khan et al. (2015). Figure 1 shows the comparison of UKESM1 modelled vertical profiles of O_3, NO_2, NO_3 and NO_3:N_2O_5 against observations made in the Eastern UK, over the North Sea, as part of the RONOCO summer campaign that took place in July 2010 (Stone et al., 2014). UKESM1 output is not constrained by meteorological forcing so we sample the model during July 2010-2014, outputting model data once every 27 hours and sampling data between 21:00 and 03:00 local time to generate a nighttime climatology for July, which is plotted in orange in Figure 1 with the error bars reflecting the variability (1 σ) in the model climatology. In general the model simulates the vertical profile of the RONOCO observations well. There is a positive bias in modelled O_3 and a negative bias in modelled NO_2 (consistent with previous analyses with UKCA the chemistry component of UKESM1 (e.g. Archibald et al., 2020b)). These biases partly offset each

https://doi.org/10.5194/acp-2022-706
Preprint. Discussion started: 16 November 2022


Atmospheric Chemistry and Physics Discussions

other; the vertical profile of the rate of production of NO_3 [Eq. 1] is in good qualitative agreement between the model and observations, with maxima found above the surface below 1 km, but the absolute magnitude of the NO_3 production rate is underestimated in the model by a factor of ~ 2 in this region. One reason for the model disagreement is likely the resolution, whereby the UKESM1 model is unable to simulate the fine plumes of NO_2 that drive NO_3 production that were observed during the RONOCO campaign (Stone et al., 2014).

https://doi.org/10.5194/acp-2022-706
Preprint. Discussion started: 16 November 2022

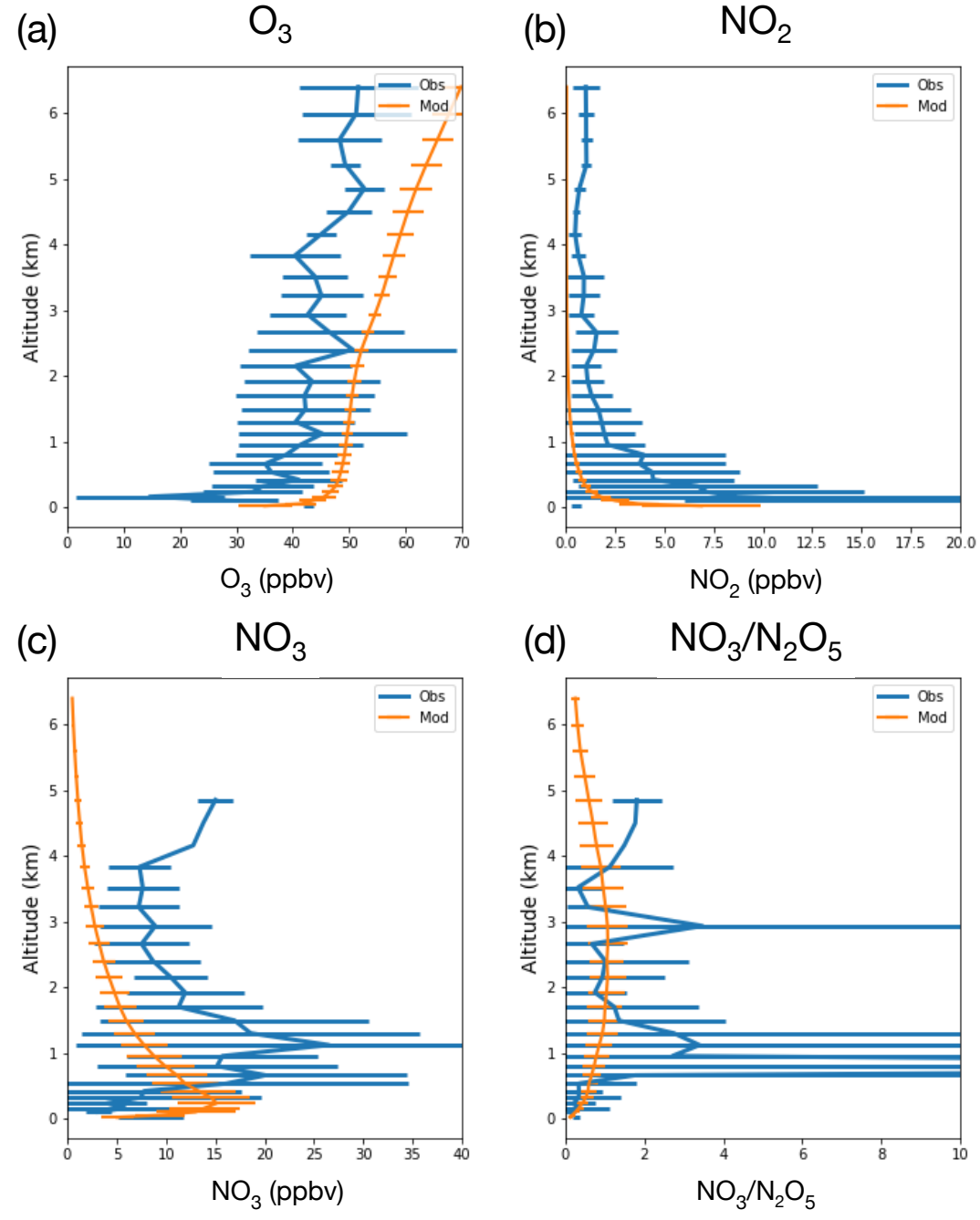

Figure 1.Comparison of vertical profile of night-time concentrations of O_3 (a), NO_2 (b), NO_3 (c) and NO_3:N_2O_5 ratio (d) between RONOCO July 2010 flight campaign and 2010-2014 July nighttime values from UKESM1 model simulations from grid cells corresponding to flight regions. Lines show means and error bars show standard deviation.

https://doi.org/10.5194/acp-2022-706
Preprint. Discussion started: 16 November 2022

Atmospheric Chemistry and Physics Discussions

Table 1 compares results from the Historical simulation of UKESM1 against the STOCHEM-CRI model data from Khan et al. (2015) and a synthesis of surface observations; see Khan et al. (2015) for details and references for observational data. Our model data are averages from the 2010-14 period corresponding to the months of each campaign and are in good qualitative and quantitative agreement with the observations (which come from a range of different techniques and cover a range of different dates over the period c.a. 1990s-2010s, see Khan et al. (2015) for details). The largest disagreement in Table 1 is at Guangzhou, China, where both models predict much lower levels of NO_3 than were observed using a long-path DOAS instrument (Li et al., 2012). Despite being of low horizontal and vertical resolution UKESM1 reproduces well current observations of NO_3 suggesting it is a suitable tool for simulating past and future changes in the NO_3 burden and distribution.

Table 1. Monthly average values from of NO_3 mixing ratios (ppt) from UKESM1 compared with review of NO_3 measurements and STOCHEM model output adapted from Table 3 in Khan et al., (2015).

Site	Start	Observed (ppt)	STOCHEM (ppt)	UKESM1 (ppt)
Lindenberg	Feb-Sep 1998	4.6	6.9	8.0
Tanus	May 2008	30±20	6.9	6.9
Jerusalem	Jul 2005–Sep 2007	27±43	9.2	11.2
Houston	Aug-Sep 2006	0-149	3.3	11.0
Shanghai	Aug-Oct 2011	16±9	16.6	8.4
Guangzhou	Jul 2006	21.8±1.8	4.7	4.4
Izu-Oshima	Jun 2004	3	4.4	7.5
Mace Head	Jul-Aug 1996	5	3.8	3.1
Canary Islands	May 1994	8±3	5	5.7
Finokalia	Jun 2001– Sep 2003	4.2±2.3	16	16.9
Weybourne	Oct-Nov 2004	6	5.5	4.2
East Point	Jul-Aug 2005	13.1	1.6	1.4
Schauinsland	Aug 1990	5.8	12	6.3

3.2 Modelled Past and Future Changes in O_3, NOx and NO_3

Our analysis focuses on five year periods from the simulations, comparing present day (PD; 2010-2014) and preindustrial (PI; 1850-1854) periods with end of century (2090-2094) predictions under four shared socioeconomic pathways (SSPs) as used

https://doi.org/10.5194/acp-2022-706
Preprint. Discussion started: 16 November 2022


Atmospheric Chemistry and Physics Discussions

for CMIP6. Data for these five year periods were collected by rerunning the UKESM1 CMIP6 simulations with additional diagnostics for analysis and corrected NO_3+MONOTERP reaction rate coefficient (see Methods section for details). The future emission pathways we studied, described in more detail in Gidden et al. (2017), are in short: SSP1-2.6, a 2˚C world with a focus on sustainability, economic growth and connectivity and low population growth driven by low-carbon technology and energy efficiency; SSP2-4.5, a middle-of-the-road scenario with slower convergence of income levels, greater population growth and reliance on fossil fuels for further into the century; SSP3-7.0, a regional rivalry scenario with increased inequality and high population growth in low-middle income countries; and SSP5-8.5, similar to SSP1 in terms of population and economic growth but driven by increasing unabated use of energy and fossil fuels. Although SSP5-8.5 leads to the greatest increase in long-lived greenhouse gas emissions, and therefore global warming, by the end of the century, SSP3-7.0 has the highest emissions of short-lived air pollutants (Rao et al., 2017). Emissions of BVOCs also change between these scenarios as they are interactive in UKESM1 (Sellar et al., 2019). BVOC emissions are higher in the PI compared to PD due to changing land use, reducing forested area over the 20th century. In the future SSP scenarios, BVOC emissions are predicted to increase as temperatures increase, in spite of the increasing CO_2 levels (which, in the absence of other changes, would cause BVOC emissions to decrease (Arneth et al., 2008)).

The results from the UKESM1 simulations show that large changes to monthly average O_3, NO_2 and NO_3 levels have taken place in the lowest km of the atmosphere from PI to PD (Fig. 2 a-c). The region of the lowest km is analysed here, rather than the surface level, because nighttime O_3 and NO_3 levels tend to be low at the surface due to rapid reaction with fresh emissions of NO and the low nighttime boundary layer. In both observations and the model, peak NO_3 tends to occur a few hundred meters above the surface (e.g. Fish et al., 1999).

The main driver for the changes between the PI and PD periods is attributed to the increase in anthropogenic emissions, with emissions of NO_x increasing by orders of magnitude over this period. The largest increases in NO_2 and O_3 occur over populated regions (Fig. 2 (a, b)). The changes in O_3 simulated with UKESM1 are in good agreement with other CMIP6 models (Griffiths et al., 2021) and show an increase in the tropospheric burden of around 40% from the PI-PD. NO_3 is similarly much higher in the PD compared to PI (Fig. 2 (c)), an increase in tropospheric burden of approximately 75%, in good agreement with previous global modelling studies (Khan et al., 2015) and with observations (see Section 2.1). To first order, NO_3 is proportional to $O_3 \times NO_2$ as these species drive its production, but there are some important deviations from this relationship. Firstly, concentrations are lower at high latitudes because colder climates mean more NO_3 is partitioned into N_2O_5. Changes in NO_3 are also supressed in regions with high BVOC emissions, such as South-East USA, South America and South-East Asia/South China, due to the high reactivity with these species. Greatest increases are over the middle East and Indian subcontinent – regions with high local temperatures, NOx emissions and O_3, as well as relatively low BVOC emissions.

https://doi.org/10.5194/acp-2022-706
Preprint. Discussion started: 16 November 2022

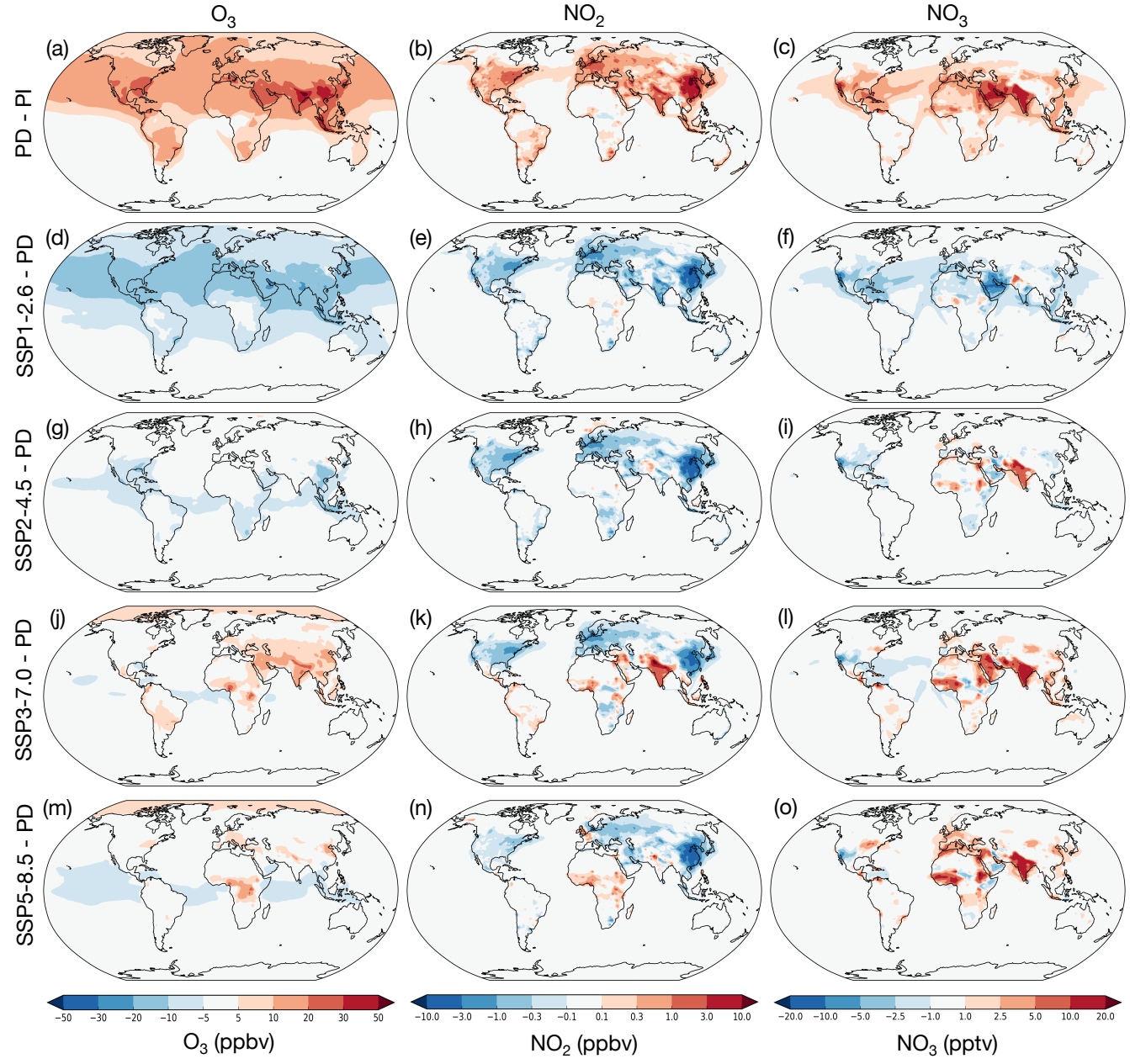

Figure 2. Changes in O_3, NO_2 and NO_3 mixing ratios averaged over lowest 1km of the atmosphere. Showing difference between Present Day (2010-2014) and Preindustrial (1850-1854) (a-c), SSP1-2.6 (2090-2094) – PD (d-f), SSP2-4.5 (2090-2094) – PD (g-i), SSP3-7.0 (2090-2094) – PD (j-l), and SSP5-8.5 (2090-2094) – PD (m-o).

220 The simulated future changes of O_3, NO_2 and NO_3 in the lowest 1km depend greatly on the future SSP scenario. Focusing on the change between the future and the PD, the SSP1-2.6 scenario shows large reductions in O_3, NO_2 and NO_3 across the world, especially in the Northern Hemisphere (Fig. 2 (d-f)). These reductions are similar to but smaller than the increases in NO_3 from

https://doi.org/10.5194/acp-2022-706
Preprint. Discussion started: 16 November 2022


Atmospheric Chemistry and Physics Discussions

the PI to PD, leading to a tropospheric NO_3 burden under SSP1-2.6 that is 26% lower than the PD burden. In SSP2-4.5 (Fig. 2 (g-i)) NO_2 decreases in most regions, although to a lesser degree in some regions such as India. However, reductions in O_3 are muted, with similar concentrations across most of the Northern Hemisphere; likely due to competing trends from changes to stratosphere-to-troposphere transport of ozone (driven by increases in the Brewer-Dobson circulation under climate change), lower NO_x emissions (decreasing ozone), and higher temperatures and BVOC emissions (increasing ozone) (e.g., Archibald et al., 2020a). Changes in NO_3 are spatially variable, with small reductions in North America and China but increasing levels in Northern Europe, India and parts of Africa. In the SSP3-7.0 scenario (Fig. 2, (j-l)), which simulates the greatest increase in emissions of short-lived pollutants, near-surface O_3 is predicted to increase over most populated regions, particularly in South Asia and West Africa. In contrast, NO_2 shows diverging trends, decreasing in North America, Europe and China but increasing considerably in India, the middle East and West Africa. Over most parts of the land and oceans NO_3 is predicted to not change significantly but specific regions show dramatic increases: by over 10 ppt in West Africa, the middle East and India (Fig. 2 (l)). These large increases in NO_3 are of a similar order to the PI-PD changes shown in Fig. 2 (c), effectively doubling near-surface NO_3 concentrations in the future over many populated regions, whilst O_3 increases are only in the order of 50% greater than the PD. In SSP5-8.5 (Fig. 2 (m-o)), the warmest future scenario, the increases in O_3 in Asia are small and NO_2 is predicted to remain similar to present day in India whilst decreasing significantly in China. However, there is still a considerable increase in NO_3 over India as well as West Africa and Europe predicted under the SSP5-8.5 scenario (in the order of 10-20 ppt increases above PD levels). These variations in trends between scenarios show that it is not sufficient to assume that lower NO_x emissions in the future will result in reduced NO_3. Rather, it is a complicated outcome also depending on other changes in the chemical environment and climate.

To investigate the role of changes in climate on NO_3, through changes in temperature over the lowest 1km of the atmosphere, the natural logarithm of K_{eq} (Equation 3) is plotted against the corresponding temperature values in Figure 3, using data from each of the scenarios. This shows the strong dependence of K_{eq}, in accordance with the Van't Hoff relationship. As the climate warms the thermal equilibrium shifts such that more N_xO_y is found as NO_3, increasing the amount of NO_3 available for oxidation and reducing the sink due to the N_2O_5 heterogeneous reactions. UKESM1 simulates levels of warming by the end of the 21st century that are at the higher end of the CMIP6 multi model mean but within the ensemble spread (Tebaldi et al., 2021).

https://doi.org/10.5194/acp-2022-706
Preprint. Discussion started: 16 November 2022

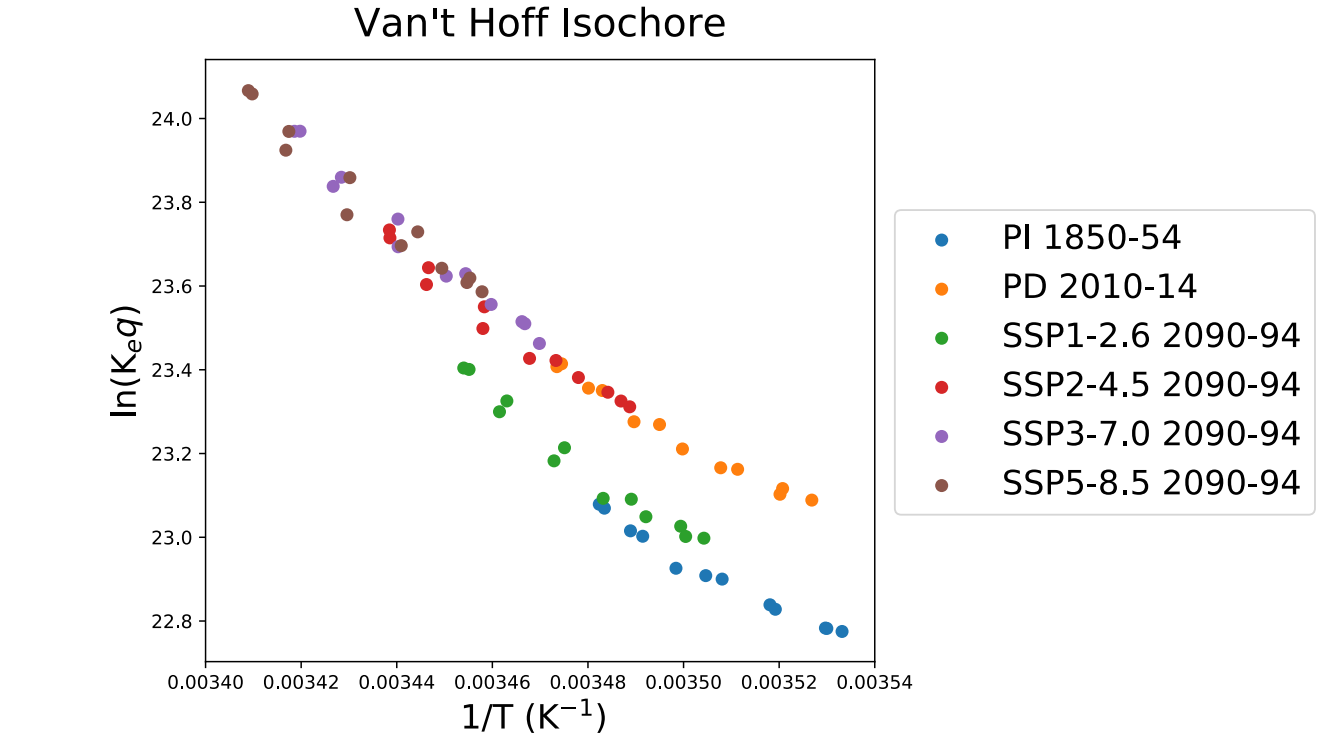

Figure 3. Van't Hoff isochore of the thermal equilibrium between NO_3 and N_2O_5 (a) and change in temperature in UKESM1 model simulations from 1850 to 2100 in four representative SSP scenarios (b) changes in temperature from historical simulation from 1850 to 2014, and along SSP scenarios from 2014 to 2100.

255

3.3 Changes to BVOC oxidation

Figure 4 shows vertically integrated modelled oxidation fluxes for isoprene and MONOTERP (the lumped monoterpene species in UKESM1) averaged across the globe and over Southern Asia (SA; defined as 5°N, 50°E to 35°N 95°E, based on the source-receptor region used by the Task Force on Hemispheric Transport of Air Pollution, TF HTAP, www.htap.org . Plots
260 for the other TF HTAP regions are included in Supplement). The modelled oxidation flux is calculated at each model chemistry timestep (1 hour), thereby taking into account the concentrations of the BVOC, oxidants and the temperature dependent rate coefficients for their reactions, then averaged over each month for analysis. The fluxes are further averaged over the lowest 1 km of the atmosphere to reflect boundary layer oxidation in Figure 4. In the PI atmosphere, NO_3 initiated oxidation accounts for less than 1% of isoprene and 4% of MONOTERP, due to the low NO_x emissions in this period (Fig. 2b). This fraction of
265 oxidation increases to 3% and 13% for isoprene and MONOTERP respectively for present day (i.e. a factor of 3 increase). UKESM1 predicts that Monoterpene emissions increase in a warming climate in all scenarios, particularly in SSP3-7.0 and

https://doi.org/10.5194/acp-2022-706
Preprint. Discussion started: 16 November 2022

Atmospheric Chemistry and Physics Discussions

SSP5-8.5. Across the whole troposphere, the relative amount via NO_3 stays the same in SSP3-7.0 relative to PD, although the absolute amount increases as BVOC emissions increase. However, over the South Asian region the fraction of MONOTERP oxidised by NO_3 increases from 13% to 15%. In SSP1-2.6, MONOTERP oxidation fraction by NO_3 decreases in all regions evaluated.

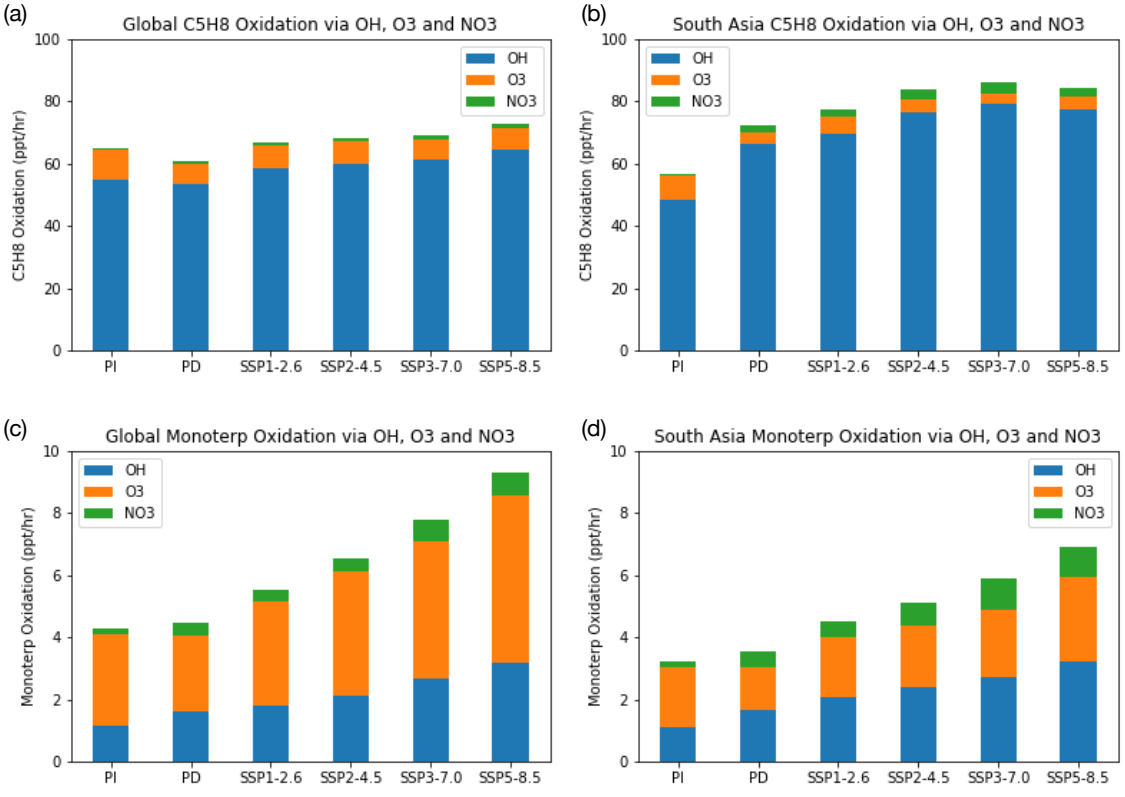

Fig. 4 Average oxidation rates in lower 1km of atmosphere for isoprene (a and b) and MONOTERP (c and d), averaged across the whole globe (a, c) and over South Asia region (b, d).

Focusing on MONOTERP oxidation, which in UKESM1 leads to the formation of SOA, Figure 5 shows the vertical profiles of the oxidation of this compound under PD conditions (panels (a) and (c)) and the SSP3-7.0 future scenario (panels (b) and (d)). Similar figures for the other SSP scenarios are included in the Supplement. As with Figure 4, Figure 5 shows that the future scenario results in an increase in oxidation of MONOTERP (an increase in SOA production in the model) for all oxidants. The vertical profiles show a sharp drop in the oxidation flux away from the surface as a result of the relatively short lifetime of the MONOTERP species, which is emitted in the model at the surface and decays away in the vertical rapidly. Focusing on the near surface, where the rate of SOA production via MONOTERP oxidation is highest, Figure 5 shows that over Southern Asia the UKESM1 model predicts an increase in near surface NO_3 oxidation of MONOTERP of a factor of 2

https://doi.org/10.5194/acp-2022-706
Preprint. Discussion started: 16 November 2022

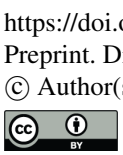

Atmospheric Chemistry and Physics Discussions

under the SSP3-7.0 scenario. This implies potential for enhanced production of organic nitrogen containing aerosols under future climate and emissions scenarios, compounds whose health and climatic effects have been hitherto less well studied but observational evidence suggests are ubiquitous in the atmosphere (Kiendler-Scharr et al., 2016).

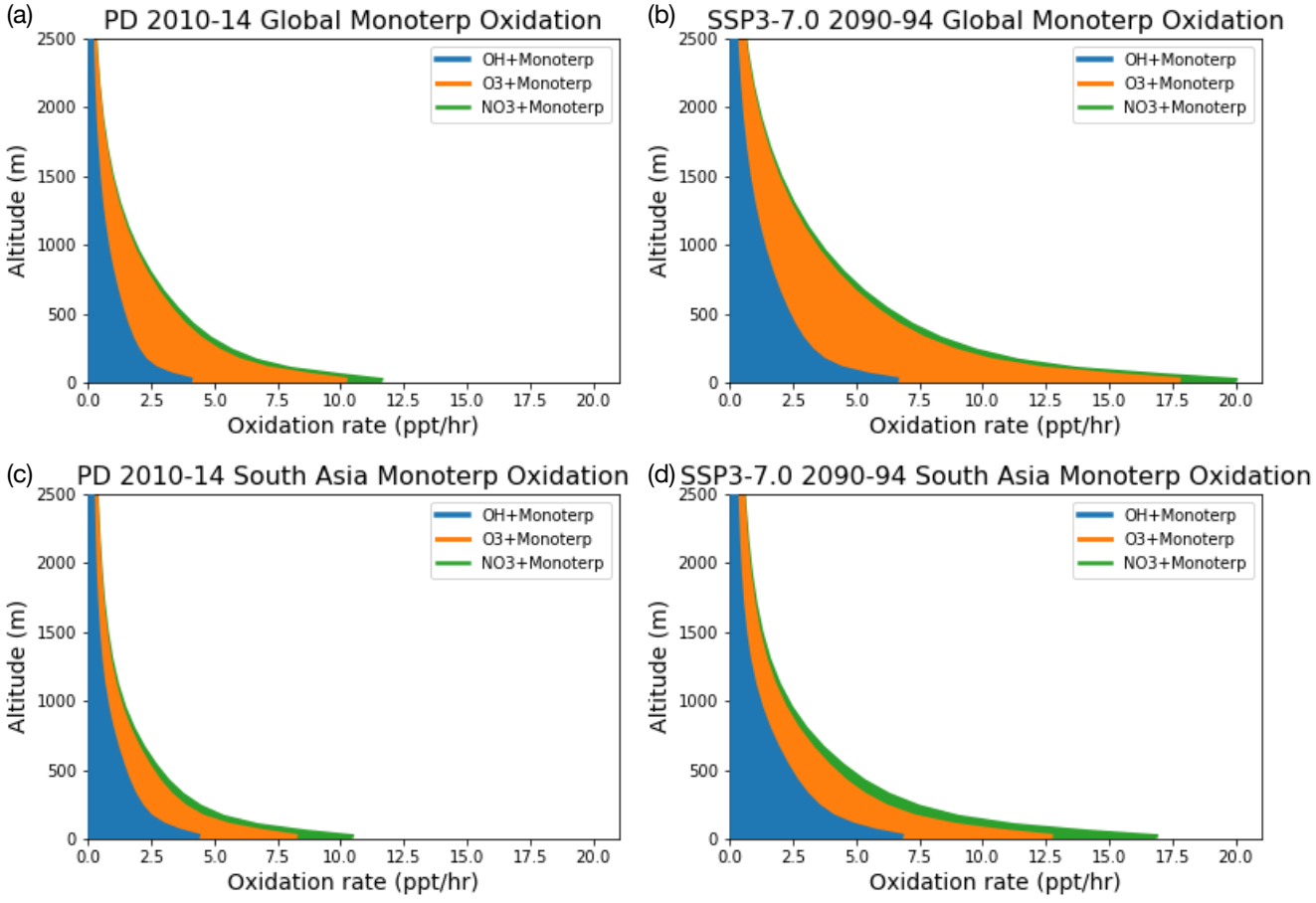

Fig. 5. Vertical profile of MONOTERP oxidation via OH, O_3 and NO_3. Panels (a) and (c) show the model calculated present day global and South Asian oxidation fluxes respectively. Panels (b) and (d) show these fluxes at the end of the 21st Century under the SSP3-7.0 scenario. The future scenario results in increases in all oxidation fluxes, with the NO_3 initiated oxidation flux increasing by a factor of 2 compared with the present day oxidation rates in South Asia.

4 Discussion

Whilst we have demonstrated large potential changes in NO_3 in the future under the SSP scenarios, we acknowledge that there are some limitations to the state-of-the-art CMIP6 models, like UKESM-1. Faithful simulation of NO_3 requires models which capture a wide range of processes as discussed in Ng et al. (2017). These include, the ability to simulate faithfully the diurnal variability of the boundary layer, which has been shown to be a challenge for these types of models in East Asia (Yue et al.,

https://doi.org/10.5194/acp-2022-706
Preprint. Discussion started: 16 November 2022


Atmospheric Chemistry and Physics Discussions

2021); Simulating the diurnal emissions of important NO_3 sinks, like isoprene (Cao et al., 2021) – which almost all interactive chemistry CMIP6 models do – and NO_3 sources, like NO_x, which no CMIP6 models do. Further work is required to improve the representation of these key emissions sources and processes in global chemistry-climate models.

5 Conclusions

In this work we have demonstrated the potential pathways for future evolution of NO_3, the most important oxidant at night, in the lower troposphere. Analysis of our model simulations against historic measurements highlights that in spite of the relatively low resolution of the UKESM1 model, it is able to capture the magnitude and variability of observations of NO_3 and its precursors (O_3 and NO_2). We have assessed four different future scenarios which span a wide range of possible NO_x and VOC emission pathways, and levels of climate change, simulated using the UKESM1 Earth system model. This is, to our knowledge, the first assessment of future simulations of NO_3 and this work highlights the potential for significant increases in this major night-time oxidant. In particularly we have shown that, depending on the emissions scenario, regions of Southern Asia are an area of particular interest with potential increases in NO_3 to unprecedented levels; more than double their present day values. We also demonstrate the importance of climate change on NO_3, and show that the ratio of NO_3:N_2O_5 is predicted to increase under the higher climate forcing future scenarios.

The potential increases in NO_3 are shown to be important in the context of enhancing the oxidation of BVOCs in the atmosphere. Due to the poorer understanding of SOA formation from NO_3 oxidation (Ng et al., 2017) than from OH or O_3 oxidation, these findings highlight the need for further lab and field studies to better understand the SOA forming potential of BVOC oxidation initiated via NO_3 and the incorporation of these data into global chemistry and Earth system models. Our simulated changes in NO_3 are likely dependent on (1) model structure, more work investigating the impacts of vertical and horizontal resolution is required; (2) emissions, including soil NOx emissions, which are highly uncertain still, and the diurnal and hebdomadal variation in anthropogenic ones – as with most CMIP6 models the emissions in UKESM1 are prescribed without diurnal variations which are likely to impact NO_3 more than other oxidants; (3) chemical processes, with simplifications in the treatment of N_2O_5 heterogeneous chemistry being a potentially key area (as discussed by Archibald et al., (2020a) in the context of ozone budgets); and (4) the chemical mechanism used, Archer-Nicholls et al., (2021) and Weber et al., (2021) show that the NO_y budget is highly sensitive to use of a more comprehensive chemical mechanism in the UKESM1 framework. Almost all CMIP6 models that have simulated interactive chemistry have simulated changes in NO_3 and we encourage the modelling community to undertake a multi model analyses similar to those focused on OH (Stevenson et al., 2020) and O_3 (Griffiths et al., 2021). Further multi model analyses are required to constrain the level of model uncertainty in predictions of NO_3 and the potential impacts this could have on future air quality and climate.

https://doi.org/10.5194/acp-2022-706
Preprint. Discussion started: 16 November 2022


Atmospheric Chemistry and Physics Discussions

References

Archer-Nicholls, S., Abraham, N. L., Shin, Y. M., Weber, J., Russo, M. R., Lowe, D., Utembe, S. R., O'Connor, F. M., Kerridge, B., Latter, B., Siddans, R., Jenkin, M., Wild, O., & Archibald, A. T.: The Common Representative Intermediates Mechanism Version 2 in the United Kingdom Chemistry and Aerosols Model. Journal of Advances in Modeling Earth Systems, 13(5), 1–37. https://doi.org/10.1029/2020MS002420, 2021.

Archibald, A.T., Neu, J.L., Elshorbany, Y.F., Cooper, O.R., Young, P.J., Akiyoshi, H., Cox, R.A., Coyle, M., Derwent, R.G., Deushi, M. and Finco, A.: Tropospheric Ozone Assessment Report: A critical review of changes in the tropospheric ozone burden and budget from 1850 to 2100. Elementa: Science of the Anthropocene, 8(1), doi: 10.1525/elementa.2020.034, 2020a.

Archibald, A., O'Connor, F., Abraham, N. L., Archer-Nicholls, S., Chipperfield, M., Dalvi, M., Folberth, G., Dennison, F., Dhomse, S., Griffiths, P., Hardacre, C., Hewitt, A., Hill, R., Johnson, C., Keeble, J., Köhler, M., Morgenstern, O., Mulchay, J., Ordóñez, C., Zeng, G.: Description and evaluation of the UKCA stratosphere-troposphere chemistry scheme (StratTrop vn 1.0) implemented in UKESM1. Geoscientific Model Development, 13, 1223–1266. Doi:10.5194/gmd-2019-246, 2020b.

Arneth, A., Niinemets, Ü., Pressley, S., Bäck, J., Hari, P., Karl, T., Noe, S., Prentice, I. C., Serça, D., Hickler, T., Wolf, A., & Smith, B. Process-based estimates of terrestrial ecosystem isoprene emissions: Incorporating the effects of a direct CO2-isoprene interaction. Atmospheric Chemistry and Physics, 7(1), 31–53. doi:10.5194/acp-7-31-2007, 2007.

Arneth, A., Monson, R.K., Schurgers, G., Niinemets, Ü. and Palmer, P.I.: Why are estimates of global terrestrial isoprene emissions so similar (and why is this not so for monoterpenes)? Atmospheric Chemistry and Physics, 8(16), pp.4605-4620, doi:10.5194/acp-8-4605-2008, 2008.

Atkinson, R., Baulch, D. L., Cox, R. A., Hampson, R. F., Kerr Chairman, J. A., & Troe, J.: Evaluated Kinetic and Photochemical Data for Atmospheric Chemistry: Supplement III. IUPAC Subcommittee on Gas Kinetic Data Evaluation for Atmospheric Chemistry. *Journal of Physical and Chemical Reference Data*, *18*(2), 881–1097. Doi:10.1063/1.555832, 1989.

Atkinson, R., & Arey, J.: Gas-phase tropospheric chemistry of biogenic volatile organic compounds: A review. Atmospheric Environment, 37(SUPPL. 2), 197–219. https://doi.org/10.1016/S1352-2310(03)00391-1, 2003.

Bianchi, F. et al. Highly Oxygenated Organic Molecules (HOM) from Gas-Phase Autoxidation Involving Peroxy Radicals: A Key Contributor to Atmospheric Aerosol. Chem. Rev. (2019). doi:10.1021/acs.chemrev.8b00395

https://doi.org/10.5194/acp-2022-706
Preprint. Discussion started: 16 November 2022


Atmospheric Chemistry and Physics Discussions

Bianchi, F., Tröstl, J., Junninen, H., Frege, C., Henne, S., Hoyle, C. R., Molteni, U., Herrmann, E., Adamov, A., Bukowiecki, N., Chen, X., Duplissy, J., Gysel, M., Hutterli, M., Kangasluoma, J., Kontkanen, J., Kürten, A., Manninen, H. E., Münch, S., Baltensperger, U.: New particle formation in the free troposphere: A question of chemistry and timing. *Science*, *352*(6289), 1109–1112, doi:10.1126/science.aad5456, 2016.

Boyd, C.M., Sanchez, J., Xu, L., Eugene, A.J., Nah, T., Tuet, W.Y., Guzman, M.I. and Ng, N.L.: Secondary organic aerosol formation from the β-pinene+ NO 3 system: effect of humidity and peroxy radical fate. Atmospheric Chemistry and Physics, 15(13), pp.7497-7522, doi:10.5194/acp-15-7497-2015, 2015.

Brewer, D. A., Ogliaruso, M. A., Augustsson, T. R., & Levine, J. S.: The oxidation of isoprene in the troposphere: Mechanism and model calculations. Atmospheric Environment (1967), 18(12), 2723–2744. https://doi.org/10.1016/0004-6981(84)90338-X, 1984.

Brown, S. S. & Stutz, J. Nighttime radical observations and chemistry. Chem. Soc. Rev. 41, 6405–47, 2012.

Cao, Y., Yue, X., Liao, H., Yang, Y., Zhu, J., Chen, L., Tian, C., Lei, Y., Zhou, H. and Ma, Y. Ensemble projection of global isoprene emissions by the end of 21st century using CMIP6 models. Atmospheric Environment, 267, p.118766. 2021.

Ehn, M., Thornton, J. a., Kleist, E., Sipilä, M., Junninen, H., Pullinen, I., Springer, M., Rubach, F., Tillmann, R., Lee, B., Lopez-Hilfiker, F., Andres, S., Acir, I.-H., Rissanen, M., Jokinen, T., Schobesberger, S., Kangasluoma, J., Kontkanen, J., Nieminen, T., Mentel, T. F.: A large source of low-volatility secondary organic aerosol. *Nature*, *506*(7489), 476–479, Doi:10.1038/nature13032, 2014.

Eyring, V., Bony, S., Meehl, G. A., Senior, C. A., Stevens, B., Stouffer, R. J., & Taylor, K. E.: Overview of the Coupled Model Intercomparison Project Phase 6 (CMIP6) experimental design and organization. *Geoscientific Model Development*, *9*(5), 1937–1958, doi:10.5194/gmd-9-1937-2016, 2016.

Fish, D. J., Shallcross, D. E., & Jones, R. L.: The vertical distribution of NO3 in the atmospheric boundary layer. Atmospheric Environment, 33(5), 687–691. doi:10.1016/S1352-2310(98)00332-X, 1999.

Fry, J. L., Kiendler-Scharr, A., Rollins, A. W., Wooldridge, P. J., Brown, S. S., Fuchs, H., Dubé, W., Mensah, A., Dal Maso, M., Tillmann, R., Dorn, H. P., Brauers, T., & Cohen, R. C.: Organic nitrate and secondary organic aerosol yield from NO3 oxidation of β-pinene evaluated using a gas-phase kinetics/aerosol partitioning model. Atmospheric Chemistry and Physics, 9(4), 1431–1449. doi:10.5194/acp-9-1431-2009, 2009.

https://doi.org/10.5194/acp-2022-706
Preprint. Discussion started: 16 November 2022

Gidden, M. J., Riahi, K., Smith, S. J., Fujimori, S., Luderer, G., Kriegler, E., van Vuuren, D. P., van den Berg, M., Feng, L., Klein, D., Calvin, K., Doelman, J. C., Frank, S., Fricko, O., Harmsen, M., Hasegawa, T., Havlik, P., Hilaire, J., Hoesly, R., Takahashi, K.: Global emissions pathways under different socioeconomic scenarios for use in CMIP6: a dataset of harmonized emissions trajectories through the end of the century. *Geoscientific Model Development*, *12*, 1443–1475, doi:10.5194/gmd-2018-266, 2019.

Gordon, H., Kirkby, J., Baltensperger, U., Bianchi, F., Breitenlechner, M., Curtius, J., Dias, A., Dommen, J., Donahue, N. M., Dunne, E. M., Duplissy, J., Ehrhart, S., Flagan, R. C., Frege, C., Fuchs, C., Hansel, A., Hoyle, C. R., Kulmala, M., Kürten, A., Carslaw, K. S. (2017). Causes and importance of new particle formation in the present-day and preindustrial atmospheres. *Journal of Geophysical Research: Atmospheres*, *122*(16), 8739–8760, doi:10.1002/2017JD026844, 2017.

Griffiths, P., Murray, L., Zeng, G., Archibald, A., Emmons, L., Galbally, I., Hassler, B., Horowitz, L., Keeble, J., Liu, J., Moeini, O., Naik, V., O'Connor, F., Shin, Y. M., Tarasick, D., Tilmes, S., Turnock, S., Wild, O., Young, P., & Zanis, P. (2021). Tropospheric ozone in CMIP6 Simulations. Atmospheric Chemistry and Physics, 21, 4187–4218. https://doi.org/10.5194/acp-2019-1216

Hantson, S., Knorr, W., Schurgers, G., Pugh, T. A. M., & Arneth, A.: Global isoprene and monoterpene emissions under changing climate, vegetation, CO2 and land use. Atmospheric Environment, 155, 35–45. doi:10.1016/j.atmosenv.2017.02.010, 2017.

Hoesly, R. M., Smith, S. J., Feng, L., Klimont, Z., Janssens-Maenhout, G., Pitkanen, T., Seibert, J. J., Vu, L., Andres, R. J., Bolt, R. M., Bond, T. C., Dawidowski, L., Kholod, N., Kurokawa, J. I., Li, M., Liu, L., Lu, Z., Moura, M. C. P., O'Rourke, P. R., & Zhang, Q.: Historical (1750-2014) anthropogenic emissions of reactive gases and aerosols from the Community Emissions Data System (CEDS). *Geoscientific Model Development*, *11*(1), 369–408, doi:10.5194/gmd-11-369-2018, 2018.

Jones, A. C., Hill, A., Remy, S., Abraham, N. L., Dalvi, M., Hardacre, C., Hewitt, A. J., Johnson, B., Mulcahy, J. P., and Turnock, S. T.: Exploring the sensitivity of atmospheric nitrate concentrations to nitric acid uptake rate using the Met Office's Unified Model, Atmos. Chem. Phys., 21, 15901–15927, https://doi.org/10.5194/acp-21-15901-2021, 2021.

Khan, M. A. H., Cooke, M. C., Utembe, S. R., Archibald, A. T., Derwent, R. G., Xiao, P., Percival, C. J., Jenkin, M. E., Morris, W. C., & Shallcross, D. E.: Global modeling of the nitrate radical (NO_3) for present and pre-industrial scenarios. *Atmospheric Research*, *164–165*(3), 347–357. Doi:10.1016/j.atmosres.2015.06.006, 2015.

430 Kiendler-Scharr, A., Mensah, A.A., Friese, E., Topping, D., Nemitz, E., Prévôt, A.S., Äijälä, M., Allan, J., Canonaco, F., Canagaratna, M. and Carbone, S.: Ubiquity of organic nitrates from nighttime chemistry in the European submicron aerosol. Geophysical research letters, 43(14), pp.7735-7744, doi:10.1002/2016GL069239, 2016.

Li, S., Liu, W., Xie, P., Qin, M., & Yang, Y.: Observation of nitrate radical in the nocturnal boundary layer during a summer
435 field campaign in pearl river delta China. Terrestrial, Atmospheric and Oceanic Sciences, 23(1), 39–48. https://doi.org/10.3319/TAO.2011.07.26.01(A), 2012.

Mann, G. W. et al. Description and evaluation of GLOMAP-mode : a modal global aerosol microphysics model for the UKCA composition-climate model. Geosci. Model Dev. 519–551 (2010). doi:10.5194/gmd-3-519-2010

440

Mulcahy, J. P., Johnson, C., Jones, C., Povey, A., Sellar, A., Scott, C. E., Turnock, S. T., Woodhouse, M. T., Abraham, N. L., Andrews, M., Bellouin, N., Browse, J., Carslaw, K. S., Dalvi M., Folberth, G., Grosvenor, D., Hardacre, C., Johnson, B., Jones, A., Yool, A. (2020). Description and evaluation of aerosol in UKESM1 and HadGEM3-GC3.1 CMIP6 historical simulations. Geoscientific Model Development.

445

McGillen, M. R., Carter, W. P. L., Mellouki, A., Orlando, J. J., Picquet-Varrault, B., and Wallington, T. J.: Database for the kinetics of the gas-phase atmospheric reactions of organic compounds, Earth Syst. Sci. Data, 12, 1203–1216, https://doi.org/10.5194/essd-12-1203-2020, 2020.

450 Monks, P. S., Archibald, A. T., Colette, A., Cooper, O., Coyle, M., Derwent, R., Fowler, D., Granier, C., Law, K. S., Mills, G. E., Stevenson, D. S., Tarasova, O., Thouret, V., Von Schneidemesser, E., Sommariva, R., Wild, O., & Williams, M. L.: Tropospheric ozone and its precursors from the urban to the global scale from air quality to short-lived climate forcer. *Atmospheric Chemistry and Physics*, *15*(15), 8889–8973. Doi:10.5194/acp-15-8889-2015, 2015.

455 Mulcahy, J. P., Johnson, C., Jones, C. G., Povey, A. C., Scott, C. E., Sellar, A., Turnock, S. T., Woodhouse, M. T., Abraham, N. L., Andrews, M. B., Bellouin, N., Browse, J., Carslaw, K. S., Dalvi, M., Folberth, G. A., Glover, M., Grosvenor, D. P., Hardacre, C., Hill, R., Yool, A.: Description and evaluation of aerosol in UKESM1 and HadGEM3-GC3.1 CMIP6 historical simulations. *Geoscientific Model Development*, *13*(12), 6383–6423, doi:10.5194/gmd-13-6383-2020, 2020.

460 Ng, N. L., Brown, S. S., Archibald, A. T., Atlas, E., Cohen, R. C., Crowley, J. N., Day, D. A., Donahue, N. M., Fry, J. L., Fuchs, H., Griffin, R. J., Guzman, M. I., Hermann, H., Hodzic, A., Iinuma, Y., Jimenez, J. L., Kiendler-Scharr, A., Lee, B. H., Luecken, D. J., Zaveri, R. A.: Nitrate radicals and biogenic volatile organic compounds: oxidation, mechanisms and organic aerosol. *Atmospheric Chemistry and Physics*, *17*, 2103–2162, doi:10.5194/acp-2016-734, 2017.

O'Neill, B.C., Tebaldi, C., Vuuren, D.P.V., Eyring, V., Friedlingstein, P., Hurtt, G., Knutti, R., Kriegler, E., Lamarque, J.F., Lowe, J. and Meehl, G.A.: The scenario model intercomparison project (ScenarioMIP) for CMIP6. Geoscientific Model Development, 9(9), pp.3461-3482, doi: 10.5194/gmd-9-3461-2016, 2016.

Pacifico, F., Folberth, G. A., Jones, C. D., Harrison, S. P., & Collins, W. J.: Sensitivity of biogenic isoprene emissions to past, present, and future environmental conditions and implications for atmospheric chemistry. Journal of Geophysical Research Atmospheres, 117(D22302), doi:10.1029/2012JD018276, 2012.

Pöschl, U., Von Kuhlmann, R., Poisson, N., & Crutzen, P. J.: Development and intercomparison of condensed isoprene oxidation mechanisms for global atmospheric modeling. Journal of Atmospheric Chemistry, 37(1), 29–52, doi:10.1023/A:1006391009798, 2000.

Pöschl, U.: Atmospheric aerosols: composition, transformation, climate and health effects. Angewandte Chemie International Edition, 44(46), pp.7520-7540, doi:10.1002/anie.200501122, 2005.

Rao, S., Klimont, Z., Smith, S. J., Van Dingenen, R., Dentener, F., Bouwman, L., Riahi, K., Amann, M., Bodirsky, B. L., van Vuuren, D. P., Aleluia Reis, L., Calvin, K., Drouet, L., Fricko, O., Fujimori, S., Gernaat, D., Havlik, P., Harmsen, M., Hasegawa, T., Tavoni, M.: Future air pollution in the Shared Socio-economic Pathways. *Global Environmental Change*, *42*, 346–358. doi.org/10.1016/j.gloenvcha.2016.05.012, 2017.

Riemer, N., Vogel, H., Vogel, B., Schell, B., Ackermann, I., Kessler, C., & Hass, H.: Impact of the heterogeneous hydrolysis of N_2O_5 on chemistry and nitrate aerosol formation in the lower troposphere under photosmog conditions. *Journal of Geophysical Research*, *108*(D4), 4144, doi:10.1029/2002JD002436, 2003.

Sakulyanontvittaya, T., Duhl, T., Wiedinmyer, C., Helmig, D., Matsunaga, S., Potosnak, M., Milford, J., & Guenther, A.: Monoterpene and sesquiterpene emission estimates for the United States. *Environmental Science & Technology*, *42*(5), 1623–1629, doi:10.1021/es702274e, 2008.

Scott, C. E., Arnold, S. R., Monks, S. A., Asmi, A., Paasonen, P., & Spracklen, D. V.: Substantial large-scale feedbacks between natural aerosols and climate. *Nature Geoscience*, *11*, 1–6. Doi:10.1038/s41561-017-0020-5, 2017.

Sellar, A. A., Jones, C. G., Mulcahy, J., Tang, Y., Yool, A., Wiltshire, A., O'Connor, F. M., Stringer, M., Hill, R., Palmieri, J., Woodward, S., Mora, L., Kuhlbrodt, T., Rumbold, S., Kelley, D. I., Ellis, R., Johnson, C. E., Walton, J., Abraham, N. L.,

Zerroukat, M.: UKESM1: Description and evaluation of the UK Earth System Model. *Journal of Advances in Modeling Earth Systems*, doi:10.1029/2019ms001739, 2019.

Stone, D., Evans, M. J., Walker, H., Ingham, T., Vaughan, S., Ouyang, B., Kennedy, O. J., McLeod, M. W., Jones, R. L., Hopkins, J., Punjabi, S., Lidster, R., Hamilton, J. F., Lee, J. D., Lewis, A. C., Carpenter, L. J., Forster, G., Oram, D. E., Reeves, C. E., Heard, D. E.. Radical chemistry at night: Comparisons between observed and modelled HOx, NO3 and N2O5 during the RONOCO project. Atmospheric Chemistry and Physics, 14(3), 1299–1321, doi:10.5194/acp-14-1299-2014, 2014.

Tebaldi, C., Debeire, K., Eyring, V., Fischer, E., Fyfe, J., Friedlingstein, P., Knutti, R., Lowe, J., O'Neill, B., Sanderson, B., Van Vuuren, D., Riahi, K., Meinshausen, M., Nicholls, Z., Tokarska, K., Hurtt, G., Kriegler, E., Meehl, G., Moss, R., Ziehn, T.: Climate model projections from the Scenario Model Intercomparison Project (ScenarioMIP) of CMIP6. Earth System Dynamics, 12(1), 253–293. https://doi.org/10.5194/esd-12-253-2021, 2021.

Tröstl, J., Chuang, W. K., Gordon, H., Heinritzi, M., Yan, C., Molteni, U., Ahlm, L., Frege, C., Bianchi, F., Wagner, R., Simon, M., Lehtipalo, K., Williamson, C., Craven, J. S., Duplissy, J., Adamov, A., Almeida, J., Bernhammer, A.-K., Breitenlechner, M., Baltensperger, U.: The role of low-volatility organic compounds in initial particle growth in the atmosphere. *Nature*, *533*(7604), 527–531, doi.org/10.1038/nature18271, 2016.

Wayne, R. P., Barnes, I., Biggs, P., Burrows, J. P., Canosa-Mas, C. E., Hjorth, J., Bras, G. L., Moortgat, G. K., Perner, D., Poulet, G., Restelli, G., & Sidebottom, H.: The Nitrate Radical: Physics, Chemistry, and the Atmosphere. *Atmospheric Environment*, *25A*(1), 1–203, doi.org/0004-6981/91, 1991.

Walters, D., Baran, A. J., Boutle, I., Brooks, M., Earnshaw, P., Edwards, J., Furtado, K., Hill, P., Lock, A., Manners, J., Morcrette, C., Mulcahy, J., Sanchez, C., Smith, C., Stratton, R., Tennant, W., Tomassini, L., Van Weverberg, K., Vosper, S., Zerroukat, M.: The Met Office Unified Model Global Atmosphere 7.0/7.1 and JULES Global Land 7.0 configurations. Geoscientific Model Development, 12(5), 1909–1963. https://doi.org/10.5194/gmd-12-1909-2019, 2019.

Weber, J., Archer-Nicholls, S., Abraham, N. L., Shin, Y. M., Bannan, T., Percival, C., Bacak, A., Artaxo, P., Jenkin, M., Khan, M. A. H., Shallcross, D., Schwantes, R., Williams, J., & Archibald, A.: Improvements to the representation of BVOC chemistry-climate interactions in UKCA (vn11.5) with the CRI-Strat 2 mechanism: Incorporation and Evaluation. Geoscientific Model Development Discussions, April, 1–52. https://doi.org/10.5194/gmd-2021-119, 2021.

Yue, M., Wang, M., Guo, J., Zhang, H., Dong, X. and Liu, Y. Long-Term Trend Comparison of Planetary Boundary Layer Height in Observations and CMIP6 Models over China. Journal of Climate, 34(20), pp.8237-8256. 2021.

https://doi.org/10.5194/acp-2022-706
Preprint. Discussion started: 16 November 2022

Zhao, D., Pullinen, I., Fuchs, H., Schrade, S., Wu, R., Acir, I.-H., Tillmann, R., Rohrer, F., Wildt, J., Guo, Y., Kiendler-Scharr, A., Wahner, A., Kang, S., Vereecken, L., and Mentel, T. F.: Highly oxygenated organic molecule (HOM) formation in the isoprene oxidation by NO3 radical, Atmos. Chem. Phys., 21, 9681–9704, https://doi.org/10.5194/acp-21-9681-2021, 2021.

Code availability

Due to intellectual property rights restrictions, we cannot provide either the source code or documentation papers for the UM. The Met Office Unified Model is available for use under licence. A number of research organisations and national meteorological services use the UM in collaboration with the Met Office to undertake basic atmospheric process research, produce forecasts, develop the UM code, and build and evaluate Earth system models. For further information on how to apply for a licence, see http://www.metoffice.gov.uk/research/modelling-systems/unified-model (last access: 1 October 2021).

Data availability

The UM data used to produce the figures are available from the Centre of Environmental Data Analysis (CEDA) (https://doi.org/TODO, Archer-Nicholls et al., 2022).

Author contribution

ATA designed the research and supervised the analysis. SAN and RA led the analysis. NLA and SAN performed the re-runs of the UKESM1 model. PTG contributed to the analysis. All authors contributed to writing the manuscript.

Competing interests

The authors declare that they have no conflict of interest.